



Rheological properties of alumina nanofluids and their implication to the heat transfer enhancement mechanism

Seokwon Kim, Chongyoun Kim, Wook-Hyun Lee, and Seong-Ryong Park

Citation: *J. Appl. Phys.* **110**, 034316 (2011); doi: 10.1063/1.3622513

View online: <http://dx.doi.org/10.1063/1.3622513>

View Table of Contents: <http://jap.aip.org/resource/1/JAPIAU/v110/i3>

Published by the [American Institute of Physics](#).

Related Articles

Poroelectric relaxation indentation of thin layers of gels

J. Appl. Phys. **110**, 086103 (2011)

Landau theory description of observed isotropic to anisotropic phase transition in mixed clay gels

J. Chem. Phys. **134**, 194904 (2011)

Structural changes of poly(N-isopropylacrylamide)-based microgels induced by hydrostatic pressure and temperature studied by small angle neutron scattering

J. Chem. Phys. **133**, 034901 (2010)

A model of transluminal flow of an anti-HIV microbicide vehicle: Combined elastic squeezing and gravitational sliding

Phys. Fluids **20**, 083101 (2008)

Development of nonaqueous polymer gels that exhibit broad temperature performance

Appl. Phys. Lett. **91**, 061929 (2007)

Additional information on *J. Appl. Phys.*

Journal Homepage: <http://jap.aip.org/>

Journal Information: http://jap.aip.org/about/about_the_journal

Top downloads: http://jap.aip.org/features/most_downloaded

Information for Authors: <http://jap.aip.org/authors>

ADVERTISEMENT

	Working @ low temperatures? Contact Janis for Cryogenic Research Equipment Click here to browse our site at www.janis.com	
---	---	---

Rheological properties of alumina nanofluids and their implication to the heat transfer enhancement mechanism

Seokwon Kim,¹ Chongyoup Kim,^{1,a)} Wook-Hyun Lee,² and Seong-Ryong Park²

¹Department of Chemical and Biological Engineering, Korea University, Anam-dong, Sungbuk-ku, Seoul 136-713, Korea

²Korea Institute of Energy Research, 102 Gajeong-ro, Jang-dong, Yoosung-ku, Daejeon 305-343, Korea

(Received 17 May 2011; accepted 9 July 2011; published online 12 August 2011)

Nanofluid is a novel heat transfer fluid prepared by dispersing nanometer-sized solid particles in a traditional heat transfer fluid for heat transfer enhancement. The microstructure investigation of nanofluids by rheological techniques shows that the particles do not exist as individual particles and nanofluids of rodlike alumina nanoparticles have a sol- or weakly flocculated gel-structure depending on particle concentration. The rate of thermal conductivity increase with concentration is faster in the sol state than in the weakly flocculated gel state. When the nanofluid becomes a strongly flocculated gel thermal conductivity remains almost the same as the pure liquid value. It is concluded that the Brownian motion plays a key role in enhancing thermal conductivity. The present study is the first report on the thermal conductivity of nanofluids with the characterized dispersion status. © 2011 American Institute of Physics. [doi:10.1063/1.3622513]

I. INTRODUCTION

Nanofluid is a novel heat transfer fluid prepared by dispersing nanometer-sized solid particles in traditional heat transfer fluids such as water or ethylene glycol to increase thermal conductivity (k) and thereby heat transfer performance. The increase is known to be as large as tens of a percent and is much larger than expected from micron-sized or larger particles. Since the first report on nanofluid¹ there have been many reports on the thermal conductivity enhancement of many different kinds of materials, enhancement mechanisms and practical applications. However there have been controversies over the amount of increase in k and sometimes even over the increase itself.² One of the reasons for the controversies should come from the fact that the nanoparticles are not easily dispersed and the status of dispersion has not been fully characterized, hence the nanofluids prepared by different research groups may not have the same dispersion status. Even though the size of individual nanoparticles is reported the real size in the suspension is not known. Transmission electron microscopy (TEM) images reported in the literatures may not represent the whole system. In most of the two step methods in preparing nanofluids, the agglomerated nanoparticles would not be disintegrated into individual particles and hence the size in the suspension should be much different from the size of the individual particle. In the following we have briefly reviewed the mathematical models on the thermal conductivity of suspension since the nanofluid is virtually a new concept in rheology community.

A theory on the thermal conductivity of a composite material was first developed by Maxwell for well-dispersed spherical particles in a continuous medium.³ This theory is called the effective medium theory. This theory predicts that

the thermal conductivity of the composite material of spherical particles, k_c , is given by the following equation:

$$\frac{k_c}{k_f} = \frac{k_p + 2k_f + 2\phi(k_p - k_f)}{k_p + 2k_f - \phi(k_p - k_f)}, \quad (1)$$

where k_p is the particle thermal conductivity, k_f is the continuous phase thermal conductivity and ϕ is particle volume fraction. In the limit of $k_p \gg k_f$ and $\phi \ll 1$, the above equation becomes $k_c/k_f \cong 1 + 3\phi$. The effective medium theory was extended to the composite of nonspherical particles by Hamilton and Crosser and is given by the following equation:⁴

$$\frac{k_c}{k_f} = \frac{\beta + (n-1) - (n-1)\phi(1-\beta)}{\beta + (n-1) + \phi(1-\beta)}, \quad (2)$$

where n is $3/\Psi$ (Ψ is sphericity), β is the ratio of thermal conductivities of solid particle and the continuous phase ($\beta = k_p/k_f$). These two models by Maxwell and Hamilton-Crosser do not take into account the heat transfer resistance at the interface, i.e., Kapitza resistance.⁵ Therefore the two models are expected to deviate as the particle size becomes smaller. This deviation can be large enough to give an even smaller k_c than k_f . Nan *et al.* generalized the Maxwell model by including the Kapitza resistance⁶ and showed that k_c can be written as follows when the dispersion is perfect, in other words, particles exist only as individual ones:

$$\frac{k_c}{k_f} = \frac{3 + \phi[2\beta_{11}(1-L_{11}) + \beta_{33}(1-L_{33})]}{3 - \phi[2\beta_{11}L_{11} + \beta_{33}L_{33}]}. \quad (3)$$

In the case of prolate spheroids with principal axes $a_{11} = a_{22} < a_{33}$, the following expressions should be inserted to the above equation:

^{a)}Electronic mail: cykim@grtrkr.korea.ac.kr.

$$L_{11} = \frac{p^2}{2(p^2 - 1)} - \frac{p}{2(p^2 - 1)^{3/2}} \cosh^{-1} p,$$

$$L_{33} = 1 - 2L_{11}, \quad p = a_{33}/a_{11},$$

$$\beta_{ii} = \frac{k_{ii}^c - k_f}{k_f + L_{ii}(k_{ii}^c - k_f)}, \quad k_{ii}^c = \frac{k_p}{1 + \gamma L_{ii} k_p / k_f},$$

$$\gamma = \left(4 + \frac{2}{p}\right) \frac{R_{Bd} k_f}{a_{11}}, \quad a_k = R_{Bd} k_f (a_k: \text{Kapitza length})$$

Recently Buongiorno *et al.*² reported the results of INPBE (International Nanofluid Property Benchmark Exercise), in which the thermal conductivity of identical samples of nanofluids was measured by over 30 organizations. The samples included aqueous and nonaqueous dispersions of alumina nanoparticles among others. In the paper it was found that the increase in thermal conductivity was within the range of the Nan's effective medium theory with interfacial resistance. But in predicting the lower limit of k_c in Buongiorno *et al.*,² the effective medium theory was applied without knowing the Kapitza resistance and an estimated and fixed value of Kapitza resistance was used regardless of samples. Since k_c is very sensitive especially for the case of nanoparticles, the estimated value of k_c by the effective medium theory in Buongiorno *et al.*² may not be correct. Actually Sample 6 of the paper showed even lower k_c than the lower bound predicted by the effective medium theory by Nan *et al.*⁶ This strongly suggests that the value used in predicting the lower bound of k_c may not be properly chosen. One important point is that the INPBE experiments have not been designed to derive a conclusion on the validness of the effective medium theory based on the scientific method which consists of the collection of data through observation and experimentation, and the formulation and testing of hypotheses. The apparent agreement between the experiment and the model is only phenomenological and the apparent agreement does not warrant that the effective medium theory should be applicable. Therefore their conclusion should not be used in determining the properness of a specific model. Another important point is that the basic assumption of perfect dispersion in Nan's model was not confirmed for the samples tested and even not considered in Buongiorno *et al.*²

In addition to the effective medium theory, several enhancement mechanisms have been suggested to take into account the increase over the effective medium theory and these are classified into three categories: liquid layering around nanoparticles;^{7,8} convection induced Brownian motion of nanoparticles;^{9,10} aggregation of nanoparticles.^{11–14} These mechanisms are reviewed in detail by Prasher *et al.*¹⁰ and Kebilinski *et al.*¹⁴ Nanofluids are colloids and therefore it is conceivable that the Brownian motion of particles should have a role in the enhancement of k . However the role of the Brownian motion has not been properly taken into account yet. In estimating the Brownian effect, for example, they have regarded the diffusion velocity of a particle in the Stokes–Einstein equation as the physical velocity.^{9,10} Since the diffusion velocity should be much smaller than the instantaneous velocity, the role of Brownian motion will be underestimated if the diffusion velocity is used. Prasher *et*

*al.*¹² combined the aggregation kinetics with the Brownian motion of the aggregate while using the equipartition velocity ($v = \sqrt{3k_B T/2m}$) as the Brownian velocity of aggregate and argued that their model was well matched to their experimental data and Xie *et al.*'s experimental data.¹⁵ However their model is based on the key assumptions of the Brownian motion of aggregate and the convective enhancement expression ($k/k_l = 1 + A \text{Re}^m \text{Pr}^{0.333} \phi$, k_l is the thermal conductivity of pure liquid, Re is Reynolds number, Pr is Prandtl number, and A and m are fitting parameters), both of which have not been verified yet. Also according to their model the aggregate size is a function of time and hence k has to be a function of time, which is contrary to the fact that k is an equilibrium property. In fact they considered the case of infinite time in predicting k to compare with the experimental data, so, strictly speaking, their model did not take into account the Brownian motion.

Brownian motion is a stochastic process. The path of a Brownian particle is a fractal and such a curve cannot be differentiable. Therefore, in the analysis of Brownian motions, only the rapidity of a particle is defined rather than the physical velocity.¹⁶ Until now there has been no rigorous analysis on the effect of Brownian motions on heat transfer characteristics except for the analysis of microstructure of copper oxide nanofluids.¹⁷ Before establishing the heat transfer mechanism in nanofluids and setting up a mathematical model, it is necessary to confirm the role of Brownian motion at least qualitatively. In this study we have investigated the microstructure of alumina nanofluids by rheological methods. From the rheological studies we have been able to confirm the role of Brownian motion in enhancing k . The present study is the first report on the role of the Brownian motion of nanoparticles in nanofluids with well characterized microstructures.

II. EXPERIMENTAL METHODS

Rod-type alumina nanoparticles (Dispal X0) were supplied from the Sasol North America Inc. The TEM image supplied from the manufacturer shows that the average length and diameter of an individual nanoparticle were 50 and 10 nm, respectively. Alumina nanofluids were prepared by dispersing nanoparticles in deionized water in a beaker while stirring for 3 h with a magnetic bar following the manufacturer's suggestion. The pH of the nanofluid was 4. A part of the nanofluid was further treated by a beads-mill (The Laboratory Batch Mill, Netzsch Co.) for 1 or 5 h at 1700 rpm. The bead size was 300 μm . Another part of the sample was sonicated for 2 h using an ultrasonicator (VCX-750 Sonic Materials Inc., 750 W, 20 kHz, 20% amplitude). To make the nanofluid a strongly flocculated gel pH was controlled noting that the van der Waals attraction between particles changes with pH.¹⁸ To increase pH a proper amount of 3.0M NaOH aqueous solution was added. To check whether sedimentation and/or change in size occur during the measurement or storage, a TurbiscanTM was used. The TurbiscanTM measures the transmission and back scattering of the incident laser light from a sample along the gravity direction with time, from which one can determine the change in particle concentration and particle size along the gravity direction with time.

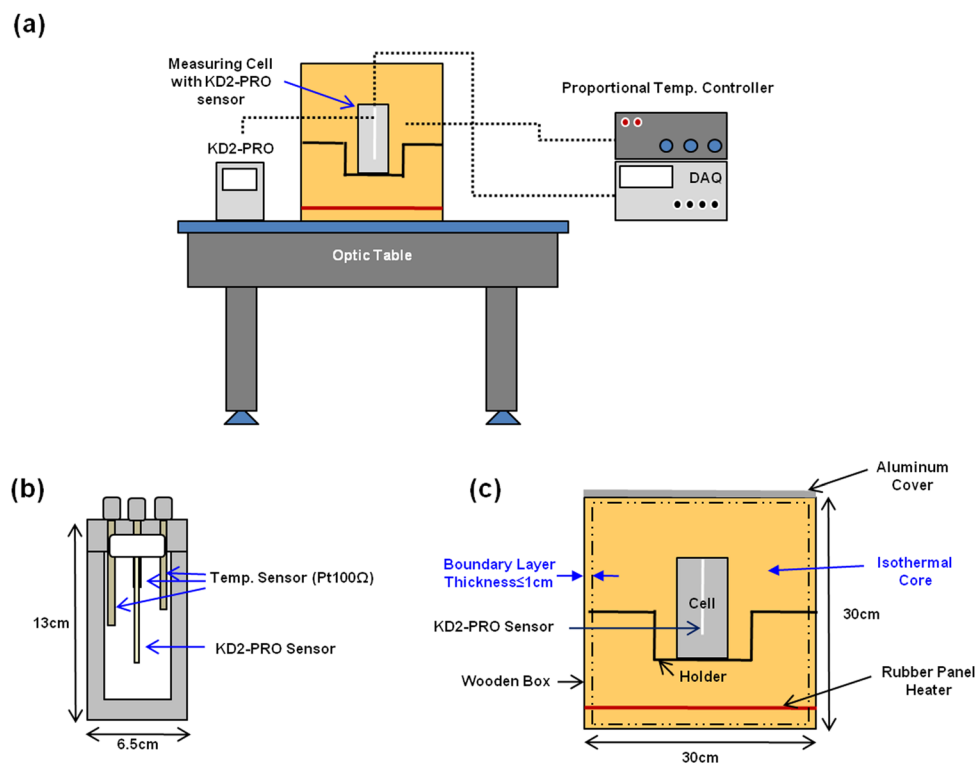


FIG. 1. (Color online) Thermal conductivity measurement system. (a) Schematic diagram of the system, (b) measuring cell, (c) environmental box.

k was measured by using a thermal conductivity meter (KD2-Pro, Decagon Devices Inc.). To minimize the effect of natural convection the probe was installed within a cell made of stainless steel as shown in Fig. 1. The cell was placed in an environmental chamber the temperature of which was controlled by a proportional controller within ± 0.1 K. The temperature within the cell was monitored at different heights and k was measured when the temperatures at different positions remained within 0.1 K. To prevent from errors due to vibration of the cell¹⁹ the environmental chamber was placed on an optical table with an air cushion.

The rheological properties of nanofluids were measured with a stress-controlled rotational rheometer (AR2000, TA Instruments). The Couette geometry (inner diameter of 14 mm, outer diameter of 15 mm) was used for viscosity measurements. The cone-and-plate geometry was used for linear viscoelastic measurement. Steady flow measurements were performed by varying shear rate. The linear viscoelastic measurements were performed after confirming the linear viscoelastic regime by strain sweep tests.

III. RESULTS

Before measuring the physical properties of nanofluids we checked sedimentation characteristics of a nanofluid ($\phi = 0.03$) with the Turbiscan. It also measures the change in average particle size with time. Figure 2 shows the scattering density variation along the gravitational direction with time. First of all, at each time lapse, the scattering (or transmission) density is almost uniform along the gravitational direction except near the meniscus region. If there is any sedimentation the transmission should increase with time at the top of the sample while the transmission should decrease with time at the bottom of the sample. The uniformity of par-

ticle concentration means that sedimentation of particles is negligibly small and particles are well dispersed for the nanofluid tested here. However the level of light transmission increases with time. This is a manifestation of the increase in the average size of particles with time. However the transmission converges to the steady value, hence the average particle size is considered to converge to the equilibrium value. It has been found that the average particle size of the aged sample is 5.7% larger than that of the fresh sample. It appears that some particles become aggregated slightly with time until the equilibrium is reached.

Figure 3 shows the viscosities of alumina nanofluids measured by the rotational rheometer. When particle volume fraction $\phi = 0.01$ or 0.02 the viscosity is a constant independent of

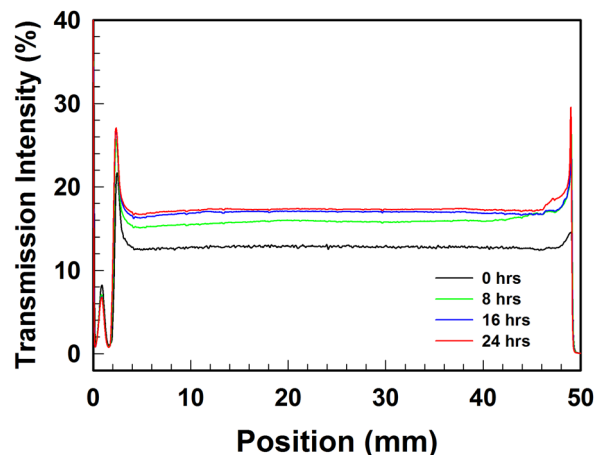


FIG. 2. (Color online) Change in light transmission with time along the gravitational direction. The height of the sample cell is approximately 45 mm. The peak at 3 mm position is due to the bottom of the glass vial and the peak at 50 mm is due to the meniscus at the air–nanofluid interface.

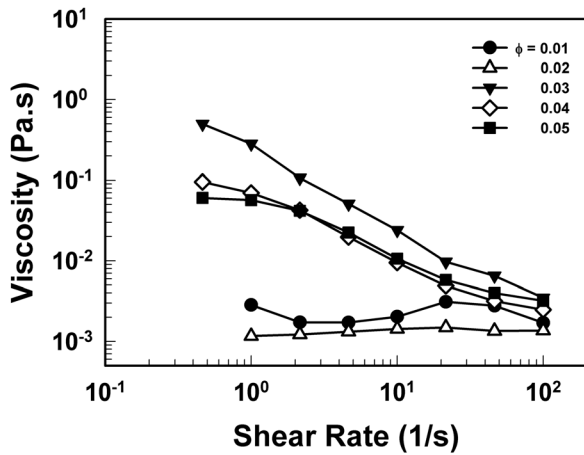


FIG. 3. Viscosity vs shear rate for alumina nanofluids with differing particle loading.

shear rate within the range of measurements. As ϕ increases from 0.02 to 0.03, the shear viscosity jumps at the low shear region ($< 10 \text{ s}^{-1}$) and becomes strongly shear thinning. When $\phi > 0.05$, the viscosity is strongly shear thinning and shear stress (viscosity times shear rate) remains approximately the same for shear rates tested here. This phenomenon is called shear banding²⁰ suggesting that the nanofluid becomes a gel in this concentration regime.²¹ Here we note that the viscosity is fluctuating and not monotonically increasing with particle loading, which is one of the typical characteristics of weakly flocculated gels. Figure 4 shows the storage (G') and loss (G'') moduli of nanofluids. When $\phi = 0.05$, G' is much larger than G'' and G' shows a plateau when ω is between 10^{-3} s^{-1} and 1 s^{-1} . These are typical characteristics of a gel material. The material has a dominantly large elastic property and the material does not relax the stress in the regime, meaning that the material would not flow. When $\phi = 0.03$, the same trend can be seen. When $\phi = 0.01$, however, both G' and G'' drop by two orders of magnitude. The elasticity is very weak and the viscosity is small, too. This is also consistent with the steady state measurement described above. We note that even at the very small value of ω , G' does not become vanishingly small. This point will be considered later.

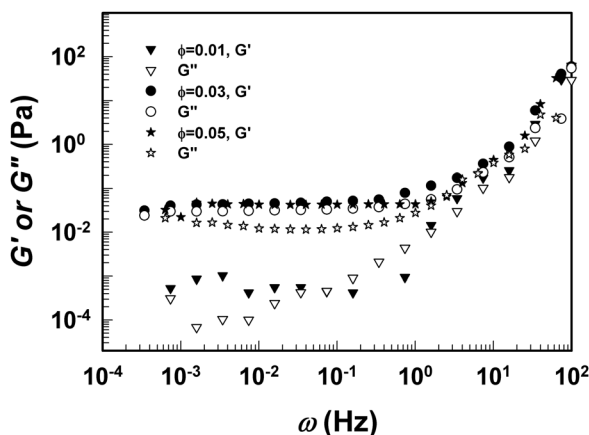


FIG. 4. Storage (G') and loss (G'') moduli of alumina nanofluids.

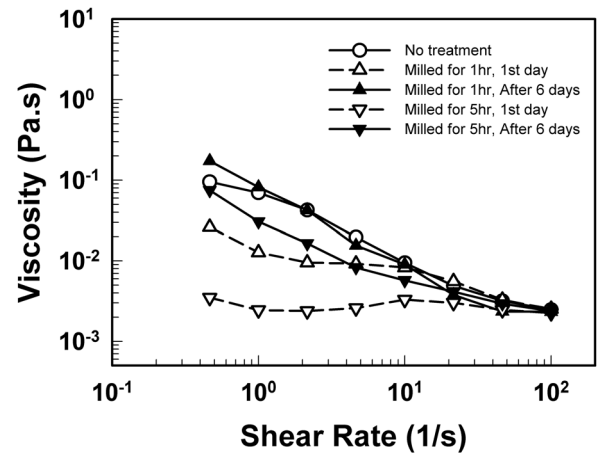


FIG. 5. The effect of the beads-mill treatment on the rheological characteristics.

The rheological measurements indicate that the alumina nanofluid forms a gel structure when ϕ exceeds 0.03 while it remains as a sol below $\phi = 0.03$. It has been known that, for weakly flocculated gels, $U/k_B T$, the ratio of the interaction energy between particles and the thermal energy is between 1 and 20.²² In this regime the Brownian motion is not fully suppressed and the Brownian motion still has some effects on particle motion. Figure 5 shows the aging effect of milled alumina nanofluids when $\phi = 0.04$. After milling viscosity is lowered by one or two orders of magnitude when shear rate is less than 1 s^{-1} and then viscosity is recovered after 6 days. This implies that the equilibrium microstructure should be broken at least partly due to the external forces and the structure is restored when no shear is imposed for a prolonged time. The constant shear stress in the low shear region and the changes in stress with time appear to indicate that the nanofluid has a network structure and this network structure breaks down by milling. Shear stresses at high shear rates remain virtually the same, which also indicates that the equilibrium microstructure is broken at this high shear stress level.

Figure 6 shows the thermal conductivity of the alumina nanofluid as a function of nanoparticle loading. It has been reported that KD2-Pro used in the present study gives

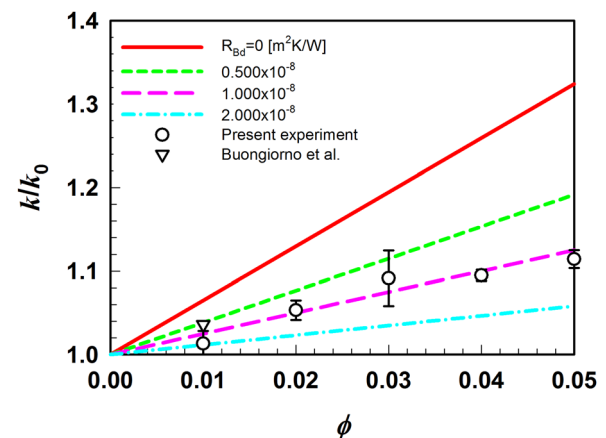


FIG. 6. (Color online) Thermal conductivity ratio (k/k_0 ; k of nanofluid/ k of base fluid) of untreated (not milled) alumina nanofluids vs particle loading. Comparison with Nan's model.

smaller values in thermal conductivity than other methods such as the transient hot wire method or the parallel plate method. This may be the reason why our data at 1% is smaller than the INPBE result which is the average of the values measured by various methods. Hence the actual k values can be possibly larger than the values obtained in the present study. Figure 6 also shows k values predicted by the effective medium theory by Nan *et al.*⁶ for different Kapitza resistance. However, as already discussed in Introduction, since the Kapitza resistance at the alumina–water interface is unknown, the exact values cannot be determined. The upper bound of the effective medium theory can be predicted when there is no Kapitza resistance. Some predicted values are also drawn for possible values of Kapitza resistance. It is noted that the predicted values are very sensitive to Kapitza resistance. This means that it is dangerous to compare the experimental results with the effective medium theory without knowing the exact value of Kapitza resistance. The present experimental results are smaller than the upper bound, but the experimental values are larger than the predicted values when Kapitza resistance is $2 \times 10^{-8} \text{ m}^2\text{K/W}$. It is not possible to tell whether the effective medium theory can be applicable or not without knowing the magnitude of Kapitza resistance. It is not intended in the present study to determine whether the effective medium theory is applied or not. Rather, in the following, it will be shown that Brownian motion plays a role in the heat flow through the alumina nanofluid. In Fig. 6 k increases almost linearly with particle loading until $\phi = 0.03$ and then k value becomes almost saturated. We can note that the crossover concentration between the linear increase and saturation and the transition concentration from the sol state to the weakly flocculated state coincide with each other. This means that at the sol state k increases faster with particle loading than at the gel state, implying that k is affected by the Brownian motion. It is noted that the fluctuation in k is much larger at particle loading of 0.03. This appears to be caused by the fluctuation of microstructure between sol and gel. Figure 7 shows the thermal conductivity of the nanofluids after the addition of NaOH when $\phi = 0.01, 0.03,$ and 0.05 . When $\text{pH} = 4$, the nanofluid shows 9% increase in k approximately in the case of the $\phi = 0.03$. But when $\text{pH} = 7$ and 11 , k decreases sharply and the amount of increase is 3% approximately.

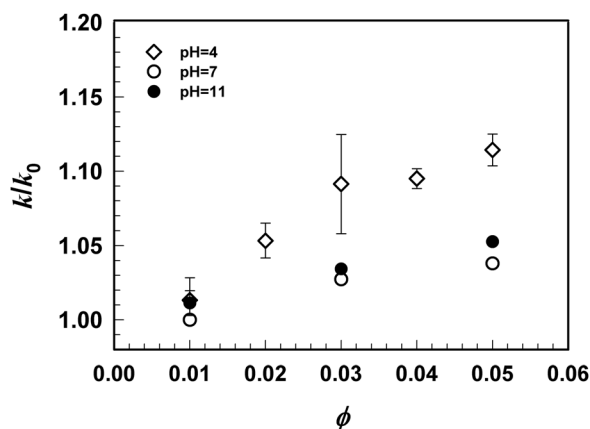


FIG. 7. The effect of pH on the thermal conductivity of nanofluids.

Figure 8 shows that the viscosity of pH controlled samples increases by more than two orders of magnitude. This means that the nanofluid becomes a strongly flocculated gel. In this strongly flocculated gel the Brownian motion of nanoparticles should be strongly suppressed. Therefore we may confirm that the suppression of the Brownian motion is responsible for the negligibly small increase in k for the flocculated sample. In Fig. 8 it is noted that k at $\text{pH} 11$ is slightly larger than k at $\text{pH} 7$. This appears to imply that the enhancement of k should not be due to the Brownian effect only and the percolation through the network should have some roles. The percolation of heat may be screened when the Brownian effect is large, but when the Brownian effect is suppressed the percolation effect can make a difference though small. The increase in viscosity with pH means the increased interparticle interaction and hence better percolation of heat. The increased effect of percolation appears to manifest itself as the increased k with viscosity at this high level of viscosity.

The present experimental results show that the enhancement characteristics are different depending on the degree of networking, in other words, the degree of arrest of individual particles by the network. This means that the aggregation of particles or the formation of networks cannot be more important than the Brownian motion in enhancing k . This also means that the percolation theory or fractal theory^{12,23,24} may not be applicable at least in the case of alumina nanofluids considered here. In the case of the sonicated sample the microstructure is destroyed at least partly by the strong shear from sonication. Therefore it will be restored when no shear is applied for a prolonged time as described above. k of the sonicated sample or milled sample is found to be much the same as the untreated sample. For example, when the particle loading is $\phi = 0.03$, the sonicated sample shows 8.5% increase in k and the 5 h milled sample shows 6.7% increase in k , both of which are close enough to the value of untreated sample of 9.0%. As the sample is subjected to sonication or milling, the microstructure is destroyed and the degree of destruction is not the same. Considering that the change in microstructure is large the change in k can be considered small. This also implies that as long as the Brownian motion should exist, the change in microstructure due to milling or sonication cannot change the heat transfer

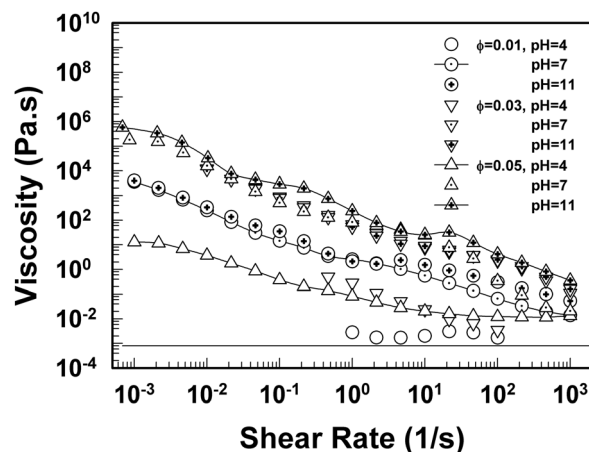


FIG. 8. The effect of pH on the rheological characteristics of nanofluids.

mechanism, supporting that the aggregation of particles or the formation of networks cannot be more important than the Brownian motion in enhancing k .

IV. DISCUSSION

In the present experimental research we first characterized the microstructure of alumina nanofluids. The series of experiments shows that there are two regimes of sol and weakly flocculated gel for the alumina nanofluids. In the sol state in which particles are subjected to Brownian motions k increases faster with particle loading than in the weakly flocculated gel state where Brownian motion is hindered at least partly. When the Brownian motion is suppressed virtually completely by changing pH , k hardly increases from the value of the dispersing fluid. k of the weakly flocculated gel shows a larger increase than the strongly flocculated gel even though the microstructures are similar to each other. The present experimental observations show that the major contribution for k enhancement should be the Brownian motion of nanoparticles for the case of alumina nanofluids of rodlike particles. Since the Brownian motion becomes more significant with the increase in temperature the role of Brownian motion should manifest itself in strong temperature dependency as reported in the literatures.^{10,23,25} The present study is the first report on the thermal conductivity of nanofluids with the characterized dispersion status.

ACKNOWLEDGMENTS

This work was supported by Energy-Resources Technology R&D Program of the Ministry of Knowledge Economy, Republic of Korea (Project No. 2008ECM11P080000). The alumina nanoparticles were donated by Dr. Yun Chang of North American Sasol Inc.

¹S. U. S. Choi, ASME FED **231/MD66**, 99 (1995).

²J. Buongiorno, D. C. Venerus, N. Prabhat, T. McKrell, J. Townsend, R. Christianson, Y. V. Tolmachev, P. Keblinski, L. W. Hu, J. L. Alvarado, I. C. Bang, S. W. Bishnoi, M. Bonetti, F. Botz, A. Cecere, Y. Chang, G. Chen, H. S. Chen, S. J. Chung, M. K. Chyu, S. K. Das, R. Di Paola, Y. L.

Ding, F. Dubois, G. Dzido, J. Eapen, W. Escher, D. Funfschilling, Q. Galand, J. W. Gao, P. E. Gharagozloo, K. E. Goodson, J. G. Gutierrez, H. P. Hong, M. Horton, K. S. Hwang, C. S. Iorio, S. P. Jang, A. B. Jarzebski, Y. R. Jiang, L. W. Jin, S. Kabelac, A. Kamath, M. A. Kedzierski, L. G. Kieng, C. Kim, J. H. Kim, S. Kim, S. H. Lee, K. C. Leong, I. Manna, B. Michel, R. Ni, H. E. Patel, J. Philip, D. Poulikakos, C. Reynaud, R. Savino, P. K. Singh, P. X. Song, T. Sundararajan, E. Timofeeva, T. Tritcak, A. N. Turanov, S. Van Vaerenbergh, D. S. Wen, S. Witharana, C. Yang, W. H. Yeh, X. Z. Zhaoand, and S. Q. Zhou, *J. Appl. Phys.* **106**, 094312 (2009).

³J. C. Maxwell, *A Treatise on Electricity and Magnetism* (Clarendon, Oxford, 1881).

⁴R. L. Hamilton, and O. K. Crosser, *Ind. Eng. Chem. Fundam.* **1**, 187 (1962).

⁵P. L. Kapitza, *J. Phys. (USSR)* **4**, 181 (1941).

⁶C. W. Nan, R. Birringer, D. R. Clarke, and H. Gleiter, *J. Appl. Phys.* **81**, 6692 (1997).

⁷W. Yu, and S. U. S. Choi, *J. Nanopart. Res.* **5**, 167 (2003).

⁸J. A. Eastman, S. U. S. Choi, S. Li, W. Yu, and L. J. Thompson, *Appl. Phys. Lett.* **78**, 718 (2001).

⁹S. P. Jang, and S. U. S. Choi, *Appl. Phys. Lett.* **84**, 4316 (2004).

¹⁰R. Prasher, P. Bhattacharya, and P. E. Phelan, *Phys. Rev. Lett.* **94**, 025901 (2005).

¹¹Y. M. Xuan, Q. Li, and W. F. Hu, *AIChE J.* **49**, 1038 (2003).

¹²R. Prasher, P. E. Phelan, and P. Bhattacharya, *Nano Lett.* **6**, 1529 (2006).

¹³W. Evans, J. Fish, and P. Keblinski, *Appl. Phys. Lett.* **88**, 093116 (2006).

¹⁴P. Keblinski, S. R. Phillpot, S. U. S. Choi, and J. A. Eastman, *Int. J. Heat Mass Tran.* **45**, 855 (2002).

¹⁵H. Q. Xie, J. C. Wang, T. G. Xi, Y. Liu, F. Ai, and Q. R. Wu, *J. Appl. Phys.* **91**, 4568 (2002).

¹⁶R. M. Mazo, *Brownian Motion* (Oxford University Press, Oxford, 2002).

¹⁷K. Kwak, and C. Kim, *Korea-Aust. Rheol. J.* **17**, 35 (2005).

¹⁸R. G. Larson, *The Structure and Rheology of Complex Fluids* (Oxford University Press, Oxford, New York, 1999).

¹⁹E. V. Timofeeva, J. L. Routbort, and D. Singh, *J. Appl. Phys.* **106**, 014304 (2009).

²⁰S. M. Fielding, *Phys. Rev. Lett.* **95**, 134501 (2005).

²¹J. K. G. Dhont, M. P. Lettinga, Z. Dogic, T. A. J. Lenstra, H. Wang, S. Rathgeber, P. Carletto, L. Willner, H. Frielinghausand, and P. Lindner, "Shear-banding and microstructure of colloids in shear flow," *Faraday Discuss.* **123**, 157 (2003).

²²W. B. Russel, D. A. Saville, and W. R. Schowalter, *Colloidal Dispersion* (Cambridge University Press, Cambridge, 1991).

²³R. Prasher, P. Bhattacharya, and P. E. Phelan, *J. Heat. Trans.* **128**, 588 (2006).

²⁴B. X. Wang, L. P. Zhou, and X. F. Peng, *Int. J. Heat Mass Tran.* **46**, 2665 (2003).

²⁵S. K. Das, N. Putra, P. Thiesen, and W. Roetzel, *J. Heat Trans.* **125**, 567 (2003).